Available online at www.sciencedirect.com
ScienceDirect
Journal of Power Sources 158 (2006) 1047–1053
JOURNAL OF POWER SOURCES
www.elsevier.com/locate/jpowsour

A study on quick charging method for small VRLA batteries

J.H. Yan [a,b], H.Y. Chen [a], W.S. Li [a,*], C.I. Wang [b], Q.Y. Zhan [b]

[a] *Department of Chemistry, South China Normal University, Guangzhou 510006, China*
[b] *Research and Design Department, B.B. Battery Co. Ltd., Raoping, Guangdong 515700, China*

Available online 6 January 2006

Abstract

It is necessary for VRLA batteries to be charged quickly in many applications. Four-step tapering current charging is utilized to study quick charging for small VRLA batteries in this paper. With the measurement of charging parameters, such as charging time, water loss, temperature rise, as well as charging efficiency, it is found that the best initial current for quick charging is within 1–1.5 CA. Then a few group of batteries are taken to conduct cyclic life testing, also a recovery charging every 30 cycles is adopted since the charging regime is partial state of charging. The result shows that a better lasting life under quick charging regime is achieved compared to that under conventional charging. Thereafter failed batteries have been torndown and analyzed, it is found that favorable connectivity among positive particles and better activity of active material is formed under quick charging regime in comparison to that under conventional charging method through SEM, XRD and other electrochemical analysis. It is also found the failure mode under quick charging regime lies in the accumulation of passivation layer at the grid interface, which results in a higher impedance and eventually capacity deterioration.

Keywords: Quick charging; Charging efficiency; Muti-step tapering current; Passivation; Failure mechanism

1. Introduction

Mas [1] has proposed an ideal charging acceptance graph in terms of minimum gassing rate on his study of gas evolution during charging for lead-acid battery. Thus, theoretical groundwork has been set up for academic research of rapid charging. According to his charging theory, very big current is permissible at the beginning of charging. Prior to battery gassing, charging efficiency maintains very well. With the charging going on, mass transport for reaction starts to cause serious polarization, and in the meantime, the polarization of electrochemical reaction goes up quickly. As a result of polarization, battery charging efficiency comes down gradually. When battery voltage goes up to the value of gassing, charging current has to be reduced to a small level in order to eliminate massive water loss. In order to keep high efficiency for rapid charging, it is a must to input as much charge as possible before gassing. Advanced Lead-Acid Battery Consortium (ALABC) has built the target for rapid charging, that is, battery must be 50% charged in less than 5 min, 80% charged in 15 min, and fully charged in 4 h [2].

There are many types of rapid charging methods being studied, all of which are aimed to reduce electrode polarization during charging and to monitor battery voltage not so high as to restrict the evolution of hydrogen and oxygen. The quick charging methods that have been studied and published in China have intermittent rest, slow frequency pulse, discharge pulse, etc. [3]. The quick charging in this paper is theoretically based on ideal charging acceptance graph, four-step tapering constant current [4] is designed in order to realize quick charging for the battery. At the first stage, the charging current is bigger than 1 CA, the charging program can be automatically changed to next one at a preset voltage so as to avoid massive water loss. At the last stage, when the battery voltage rises to 15 V, the charging is halted.

2. Experimental

2.1. Batteries

Small VRLA battery, 12 V, 7 Ah/C_{20}, the capacity of 3 C discharge is 3.3 Ah, flat paste type, AGM technology, case material is ABS.

* Corresponding author. Tel.: +86 20 85211368; fax: +86 20 85216890.
E-mail address: liwsh@scnu.edu.cn (W.S. Li).

0378-7753/$ – see front matter © 2005 Elsevier B.V. All rights reserved.
doi:10.1016/j.jpowsour.2005.11.016

2.2. Testing methods and equipment

Cyclic testing and all the charging including rapid charging are carried out at the ambient temperature of 25 ± 5 °C. Temperature on the surface of battery case is automatically recorded by thermometer mounted in Bitrode LCN circuits. Prior to charging, all the batteries are fully charged according to conventional charging as constant voltage of 14.7 V, limit current of 0.3 CA. When the charging is completed, the battery is discharged with 3 C (A) once again to confirm the resumed capacity; charging efficiency under each charging regime can be calculated accordingly.

Multi-step tapering current charging method [5] has been proposed for the research of quick charging. Each step is automatically converted at the point of 15 V. On cyclic testing, the discharge current is 3 C at final voltage of 10.5 V. For the sake of comparison, cycle life testing under conventional charging is carried out as well. In order to identify failure modes of batteries under all sorts of charging, scan electron microscopy (model Hitachi S-3000N) and X-ray diffraction (model Rigaku D/MAX-2100/PC) are utilized to observe the morphology and pattern of its microstructure of active material after failure. Electrochemical behaviour (model Autolab/PGSTAT-30) determination methods, such as cyclic voltammetry and linear sweep voltammetry, are used to characterize the activity of active material and the physical feature of corrosion layer.

3. Results and discussion

3.1. Single-step constant current charging

To understand the effect of single-step constant current for small VRL A batteries, a variety of charging currents are used to compare by 0.1 C, 0.2 C, 0.3 C, 0.5 C, 0.8 C, 1 C, 2 C, 3 C and 4 C (A) charging. Prior to charging, battery capacity is checked by 3 C discharge. After that, batteries are charged under constant current with different amperage. Once again the battery capacity is checked with 3 C discharge. Figs. 1 and 2 present the voltage profile under various charging regimes. Battery voltage control is critical on quick charging since gases start to evolve at

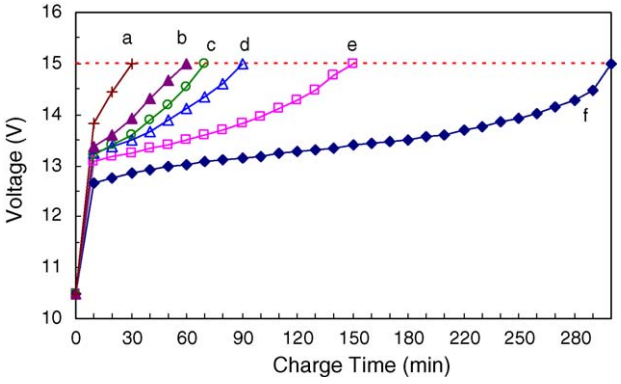

Fig. 1. Voltage profile under charging regimes ranged from 0.1 C to 0.8 C, terminated at 15 V. a, 0.8 C; b, 0.5 C; c, 0.4 C; d, 0.3 C; e, 0.2 C; f, 0.1 C.

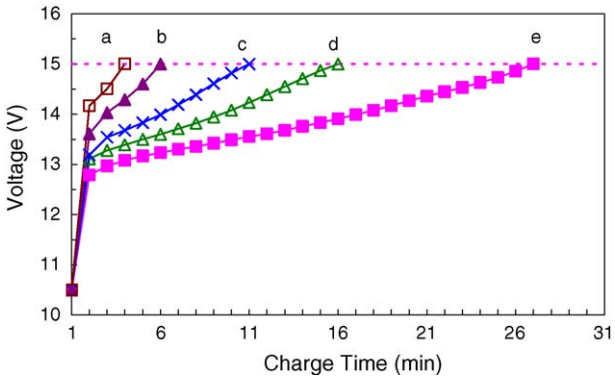

Fig. 2. Voltage profile under charging regimes ranged from 1 C to 4 C, terminated at 15 V. a, 4 C; b, 3 C; c, 2 C; d, 1.5 C; e, 1 C.

2.40 V/cell. When the charging voltage goes up to 2.60 V/cell, a lot of gases are generated inside battery cells; at the same time, the temperature inside cells ascends very quickly. In this paper, the terminated voltage is set up at 2.5 V/cell. To ensure if it is reasonable, battery weight loss is checked by a balance with accuracy 0.1 g. Almost no weight loss is found when the terminated voltage is 2.50 V/cell. The larger the charging current is, the less the time to reach the changeover voltage is. At the same discharged state, it takes 300 min for 0.1 C charging when open-circuit voltage comes to 15 V, yet it takes only a few minutes for 4 C constant current charging.

Fig. 3 shows that charged capacity depends heavily on charging current. The larger the charging current is, the quicker the voltage of battery rises and the less capacity is being charged. It can be seen that fully charged state can be realized for small current charging as 0.1 C and 0.2 C; however, it takes quite a long time, which can not meet the demand of quick charging. Fig. 4 shows that when large current charging, such as 1.5 CA, can make battery (about 45% depth of discharge) 80% charged in 15 min, and larger current of 3 C charging can make battery 50% charged in 5 min. This proves that small VRLA battery has very good charging accepatance under high current charging. As long as the appropriate charging regime is able to significantly reduce polarization, rapid charging can practically come into use for small lead-acid batteries. Chang [6] has carried out

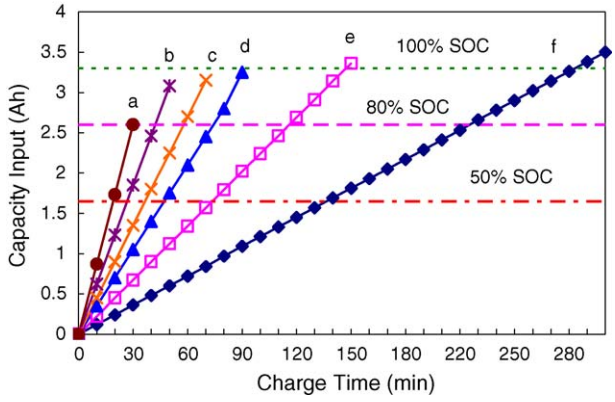

Fig. 3. Charged capacity profile under charging regimes ranged from 0.1 C to 0.8 C. a, 0.8 C; b, 0.5 C; c, 0.4 C; d, 0.3 C; e, 0.2 C; f, 0.1 C.

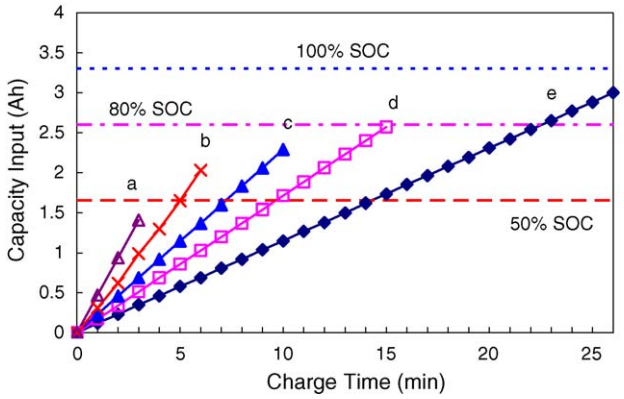

Fig. 4. Charged capacity profile under charging regimes ranged from 1 C to 4 C. a, 4 C; b, 3 C; c, 2 C; d, 1.5 C; e, 1 C.

quick charging research for many types of batteries, the result is especially optimistic for spiral battery.

3.2. Multi-step quick charging

Section 3.1 shows that single-step large current charging is difficult for battery to reach highly charged state. To achieve the aim of charging batteries quickly, some measures must be taken to reduce the voltage polarization. Hence, multi-step tapering current charging is introduced. The current at the first step is initiated from 1 C to 4 C, the second step is reduced with 0.25–0.5 C, the last step is finalized with 0.1 C. In each step, a pause of 5 min is designed in order to decrease the speed of temperature rise, as well as to depolarize the positive and negative electrodes through providing sufficient time for acid diffusion and mass transport. The charging programs are listed in Table 1; it is a kind of tapering current charging mode. There are four steps for each quick charging regime. Among each step, there is a pause of 5 min.

Fig. 5 is the typical profile of 1 C quick charging mode which depicts battery voltage, charging current and charged capacity in the course of charging. In the first 25 min, 3.02 Ah has been input, it is nearly 90% of discharged capacity. In the consequent charging steps with 0.5 C, 0.25 C, 0.1 C, input capacity declines gradually, whereas they are necessary for overall charging process. For this case, the charging program takes 62 min totally, charged capacity during the period is 3.56 Ah. The charging factor is 1.06, charging efficiency is 98.6% which is quite satisfying for its charging acceptance in a very short time.

Fig. 6 indicates that battery can be charged over 100% of the discharged volume under all kinds of quick charging ranged

Table 1
The charging programs of multi-steps tapering constant current regime

Charge step (C)	1 (A)	2 (A)	3 (A)	4 (A)
1	7	3.5	1.75	0.7
1.5	10.5	5.25	2.1	0.7
2	14	7	2.1	0.7
3	21	10.5	3.5	0.7
4	28	14	3.5	0.7

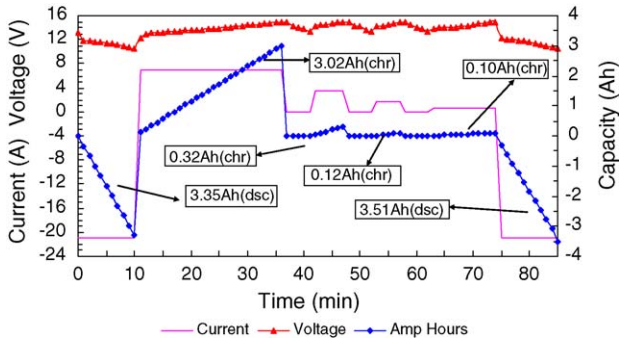

Fig. 5. A typical four-step quick charging profile starting with 1 C amperage.

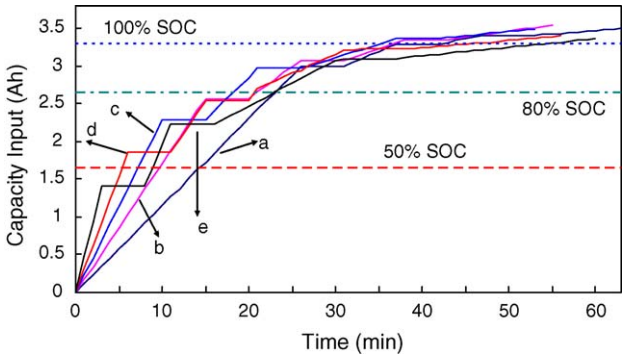

Fig. 6. Charge input profiles of all quick charging regimes after 3 C discharge. a, 1 C; b, 1.5 C; c, 2 C; d, 3 C; e, 4 C.

from 53 min to 62 min. The charging time is shortest under 2 C quick charging regime, while the most charge has been input under 1 C charging mode.

Fig. 7 is the temperature history profile on quick charging. It is found that the highest temperature rise is about 10 °C. Usually the heating generation is related to the charging current; however, it is not always the case that large current charging will result in higher temperature rise since most heat is generated at the first and second step, where heat accumulation is associated to charging time.

Charging factor and efficiency are important parameters to justify if a battery has good charging acceptance ability. In this paper, charging factor is defined as the ratio of charged volume/discharged volume. Table 2 is a contrast list of single-step

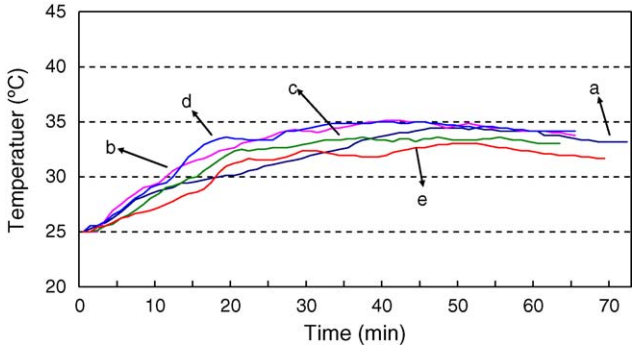

Fig. 7. Temperature rise under various quick charging regimes after 3 C discharge. a, 1 C; b, 1.5 C; c, 2 C; d, 3 C; e, 4 C.

Table 2
Charging efficiency and factor of all constant current charging regimes

Regime	Released (Ah)	Input (Ah)	Output (Ah)	Efficiency (%)	Factor	Time (min)
Single-step constant current (CA)						
0.1 C	3.34	3.50	3.45	103.0	1.05	300
0.2 C	3.37	3.38	3.35	99.4	1.00	150
0.3 C	3.39	3.25	3.26	96.1	0.96	90
0.4 C	3.38	3.15	3.17	93.8	0.93	70
0.5 C	3.36	3.08	3.15	93.7	0.92	50
0.8 C	3.41	2.62	2.85	83.5	0.77	30
Multi-step quick charging (CA)						
1 C	3.35	3.56	3.51	104	1.06	62
1.5 C	3.35	3.50	3.45	103	1.04	55
2 C	3.41	3.48	3.47	102	1.02	53
3 C	3.36	3.41	3.40	101	1.01	56
4 C	3.34	3.38	3.36	100	1.01	60

CC charging and muti-step quick charging, all the charging is terminated when battery voltage increases to 15 V. It can be seen that the charging time by single-step charging is distinct with each other, the more the charging current is, the less the charging factor and efficiency is. When charging current exceeds 0.2 CA, the charging efficiency comes down quickly and charging factor decreases to below 1.0 which represents insufficient charging. While for the multi-step quick charging, almost all the programs can make new batteries 100% charged; the charging factor is especially higher for 1 C four-step quick charging. From this table, it is also found that charging time for quick charging is not of big difference despite of the charging current.

3.3. Cyclic life testing

In order to obtain the influence of quick charging on the battery cyclic life, batteries are cycled under these conditions including conventional one. When the last capacity of batteries reaches 50% of initial one, then batteries can be regarded as failed. 14.7 V CV charging is used for conventional charging, the maximum current is 0.3 CA, charging time is about 10 h. Four-step tapering current charging regime is used to run cycles for quick charging; there is a pause of 5 min every step. The current at the first step is 1 C and 2 C, respectively. For 1 C, battery is fully charged by conventional charging every 30 cycles. For 2 C, there are two conditions for comparison, one of which is to add a subsidiary charge every 30 cycles, the other one is running without any recovery charging in the course of cycling test. Fig. 8 gives the cycling curve under all the charging modes, the result shows that 1 C/30 > 2 C/30 > 0.3 C CV > 2 C without subsidiary charging. It can be seen that battery owns very good cycling under quick charging with subsidiary charging every 30 cycles rather than that under conventional charging. Battery capacity is resumed right away once subsidiary charing is applied, while the capacity of the battery without recovery charging declines consecutively. This tells that quick charging is not 100% charged, and it is necessary to impose recovery charging on application.

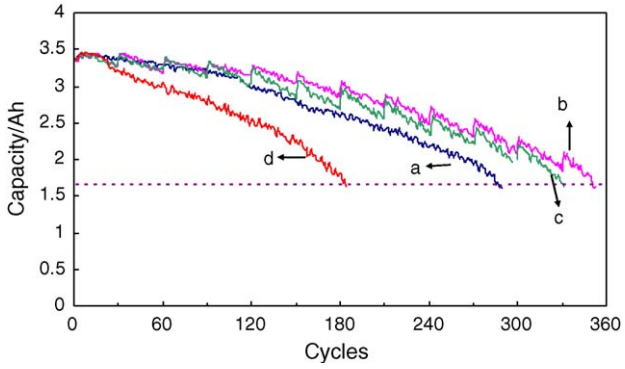

Fig. 8. Cycle life curve for quick charing and conventional charging program. a, 0.3 C CV; b, 1 C/30 quick charging; c, 2 C/30 quick charging; d, 2 C without subsidiary charging.

3.4. Failure mechanism analysis

After cycling, all failed batteries are taken to measure weight lost. By calculation, the percentage of water lost of 0.3 C, 1 C/30, 2 C/30 and 2 C/no recovery charging are, respectively, 1.3%, 1.8%, 1.6%, 1.2%, which reveals that the water lost is very marginal and it does not have any relation with the failure. Then all failed batteries are torn down; it is found that acid absorption in AGM separator is wet and sufficient, which conforms to the weight analysis. Next all plates are visually inspected to see if negative plates has been hardened, since it is signal of contraction of BET surface area.

The positive plates have to be observed if evident softening happenes. Also the grid, one of part of battery plates must be given attention if the grid corrosion is heavy or slight. To understand the failure mechanism, active material and grid electrode are taken from the samples to make further diagnoses by methods of SEM, XRD, LSV and CV.

3.4.1. SEM images

Figs. 9 and 10, respectively show SEM images of PAM and NAM, grid surface and interface. It is found that there is high porosity and good connectivity among negative particles under quick charging, while the NAM looks like contraction presenting low porosity, and their particles distributes with disordered configuration after cycled under conventional charging. In addition, the microstructure of PAM shows the morphology difference. The particles cycled under quick charging are uniform in diameter, they combine tightly each other, their agglomerates are fine in gel form. The skeleton of PAM is solid and they are connected into a rigid net with high porosity and BET surface area. While the particles cycled under conventional charging are coarse and irregular in diameter, the connectivity is loose, their agglomerates are easy to shed off due to their bad combination, which result in the failure of battery. Pavlov et al. [7] has confirmed that large current charging is benefical to the shaping of solid skeleton for PAM; in that case the cycle life under large current charging is prolonged. Fig. 9 also points out the difference between 2 C/no recovery charging and 2 C/30 quick charging mode. For 2 C quick charging without recovery charging, a lot of $PbSO_4$ is accumulated inside acive material,

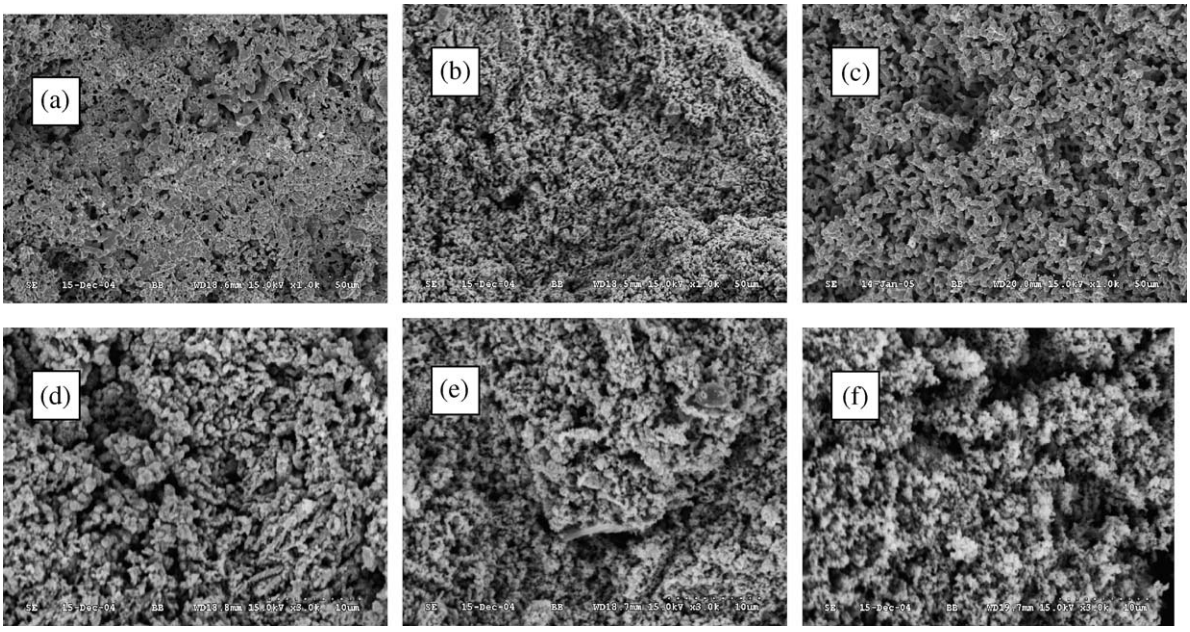

Fig. 9. SEM morphology of positive and negative AM under quick and conventional charging. a, 0.3 C (NAM); b, 2 C (NAM); c, 2 C/30 (NAM); d, 0.3 C (PAM); e, 2 C (PAM); f, 2 C/30 (PAM).

the inconvertible substance can cause bad influence on battery performance.

The passivation of corrosion layer may result into premature capacity loss since the component and structure of corrosion layer has direct influence on mechanical connection and conductivity of active material. Fig. 10 shows the existence of $PbSO_4$ on the surface and interface of grid. Under conventional charging, the particles of $PbSO_4$ are less but larger [8]; in contrast, there are massive and dense but small $PbSO_4$ formed under quick charging. Especially for the quick charging without recovery charging, the corrosion layer is quite dense. Due to the high impedance of $PbSO_4$, the conductivity of interface is impaired, which results in the failure of batteries. This is the main failure mechanism of 2 C charging without recovery charging. For the other quick charging mode with regular recovery charging, $PbO{\cdot}PbSO_4$ (BS) is found on the grid interface. The cause is that chemical reaction firstly takes place in the vicinity of grid, the acid does not catch much time to diffuse out due to the quick charging. At this moment, the electrolyte on the grid interface is strong acidic, which facilitates to generate

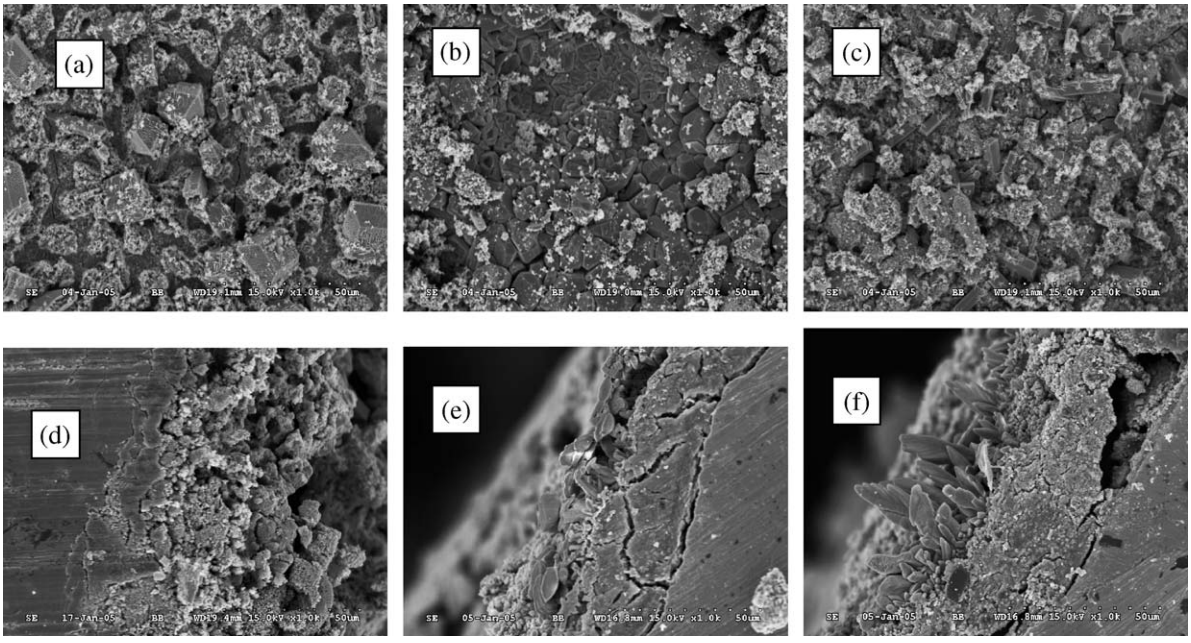

Fig. 10. SEM morphology of grid surface and interface under quick and conventional charging. a, 0.3 C surface; b, 2 C surface; c, 2 C/30 surface; d, 0.3 C interface; e, 2 C interface; f, 2 C/30 interface.

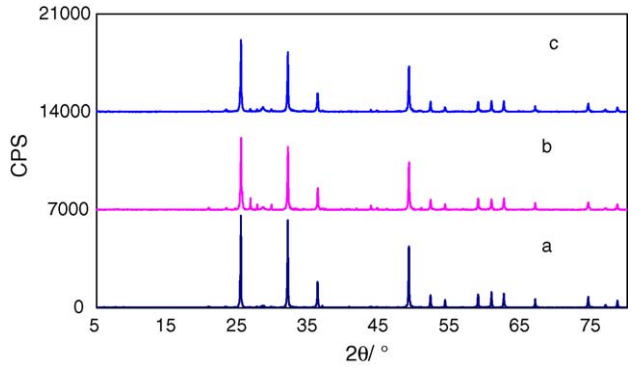

Fig. 11. XRD patterns of PAM under quick and conventional charging. a, 0.3 C CV charging; b, 2 C quick charging without recovery charging; c, 2 C quick charging with recovery charging every 30 cycles.

high density of $PbSO_4$ layer, following with the accumulation of BS.

3.4.2. X-ray diffraction analysis

Fig. 11 gives the XRD patterns of PAM cycled under conventional and quick charging regime. The characteristic peak of β-PbO_2 emerges at the same angle for two charging mode, and the characteristic peak of α-PbO_2 appears very weak. β-PbO_2 peak under conventional charging has very strong intensity, which indicates that the crystals has high crystal intergrity after cycling. Therefore, the acitivity of PAM is weak due to the recrystallization and partially aged after cycling. Meanwhile, high intensity of $PbSO_4$ exists on the battery cycled under 2 C quick charging without recovery charging, which is same as the findings from SEM images.

3.4.3. Linear scan voltammogram

LSV is used to study the feature of substance retained on corrosion layer. By analyzing the height and potential of reductive peak, the component and thickness of corrosion layer can be identified. In this experiment, a small fraction of grid is sampled from failed batteries, its surface area is about 0.53 cm^2. Prior to testing, the grid electrode is soaked into pure water for more than 30 min and is cleaned by ultrasonic sound passed through water. The electrode working system comprises three parts: reference electrode Hg/Hg_2SO_4, counter electrode Pt, and working electrode. The electrolyte (H_2SO_4) density is 1.280 g cm^{-3}, the scan speed is 1 mV s^{-1}, scan scope is from −0.4 V to −1.4 V.

Fig. 12 is the LSV of positive grid taken from failed batteries cycled under conventional and quick charging regime, respectively. The reductive peak shows the reaction from $PbSO_4$ reduced to Pb. Under conventional charging, the peak height is lower but the width is broad, its potential drifts negative. Under quick charging regime, its reductive peak is slim but stronger. The slim and strong peak indicates that passivation layer is mainly inclusive of $PbSO_4$, which is fine on size and dense on thickness. From peak curve 2, PbO is found at corrosion layer. Since $PbSO_4$ and PbO are both non-conductivity substance, battery performance will be impaired due to their existence [9]. SEM images of Fig. 10 has showed that the corrosion layer under quick charging regime is dense, which leads to higher impedance and quicker voltage drop once discharged.

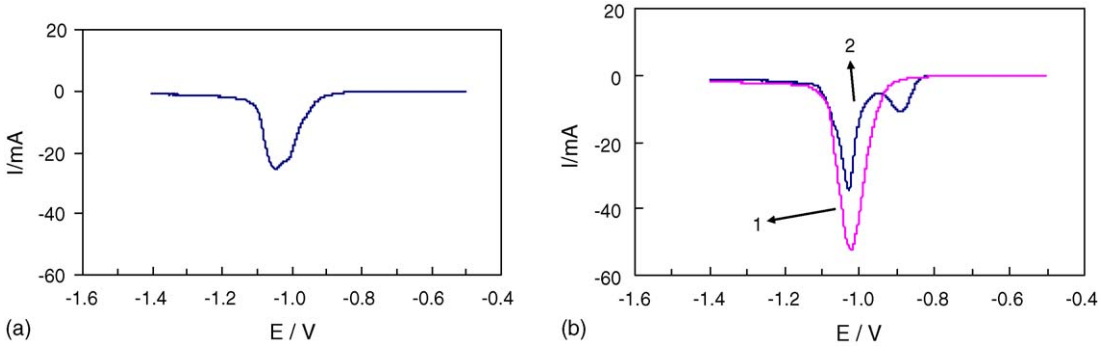

Fig. 12. LSV of positive grid taken from failed batteries after cycling. a, conventional charging; b, quick charging. (1) 2 C without recovery charging; (2) 2 C with recovery charging every 30 cycles.

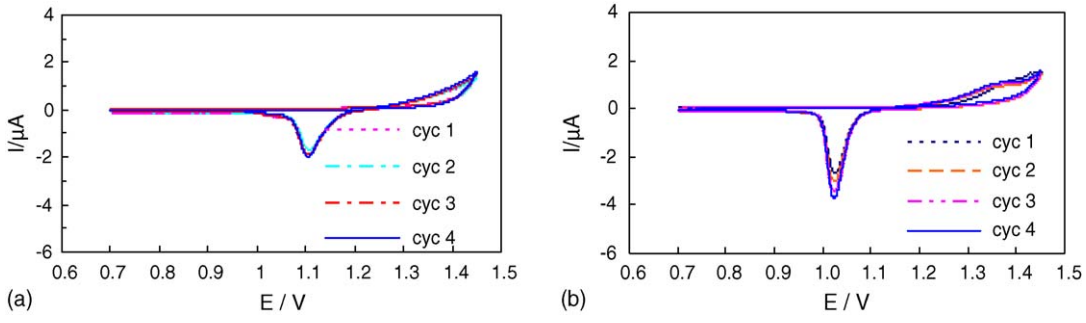

Fig. 13. Cyclic voltammogram of positive material of failed batteries after cycling. a, 0.3 C CV charging; b, 2 C quick charging with recovery charging every 30 cylces.

3.4.4. Cyclic voltammogram

To understand the activity of PAM, powder electrode is made to carry out cyclic voltammogram testing. The electrode system is identical to that working for LSV, scan speed is 2 mV s^{-1}, the scan scope is from 0.7 V to 1.45 V, consecutive four cycles are tested in this experiment.

Fig. 13 shows that the reductive and oxidative peak current is quite weak for the PAM under conventional charging. The four cylces almost overlap each other, which presents the low activity of positive material. While for PAM cycled under quick charging, strong reductive and oxidative peaks are found in the cycling, the latter reductive peak is increased in comparison to previous one. The anaylysis proves that PAM owns high reactive ability from the failed battery cycled under quick charging.

4. Conclusions

By making use of multi-step tapering current charging technology, high charging efficiency can be obtained. For small type VRLA battery studied in this paper, it is found that four-step (1–1.5) CA quick charging is most beneficial to capacity recovery and cyclic life of batteries. Through cycling life testing, it is also found that the cyclic performance under quick charging regime is better than that under conventional charging. However, it must be noted that quick charging regime still is the kind of partial state of charging and it is necessary to implement a full charging at regular intervals. Otherwise battery performance will become impaired due to incomplete charging.

The failure mode under quick and conventional charging regime is likewise different from each other. Under conventional charging, the failure is caused by softening of PAM and low activity of NAM due to the contraction of BET surface area. Under quick charging regime, it is favorable to shape uniform microstructure for positive active material, which owns higher BET surface area and activity accordingly. The main failure mode under quick charging lies in the form of dense passivation layer on the grid surface which gives rise to high impedance and acts as the obstacle for current conductivity. Finally, since the positive material cannot be fully utilized, battery becomes failed as a consequence.

Acknowledgements

This work was financially supported by National 863 Project of China (2003AA302410), NSFC (20373016), EYTP of MOE, Key Project of CISTC, MOST (2005DFA60580), International Cooperation Project of Guangdong Province (2005B50101003).

References

[1] J.A. Mas, Proceedings of the Second International Electric Vehicle Symposium, 1971, pp. 223–246.
[2] P.T. Moseley, Research results from the Advanced Lead-Acid Battery Consortium point the way to longer life and higher specific energy for lead/acid electric-vehicle batteries, J. Power Sources 73 (1998) 122.
[3] S.R. Zhu, Action of electromigration in the charge process, Battery Bimonthly 33 (2003) 169.
[4] T.X. Chen, Multi-step current and intermittent fast charging, Battery Bimonthly 27 (1997) 266.
[5] T. Ikeya, N. Sawada, et al., Multi-step constant current charging method for electrical vehicle, valve-regulated, lead/acid batteries during night time for load-levelling, J. Power Sources 75 (1998) 101.
[6] T.G. Chang, Rapid partial charging of lead-acid batteries, J. Power Sources 64 (1997) 103–110.
[7] D. Pavlov, G. Petkova, M. Dimitrov, et al., Influence of fast charge on the life cycle of positive lead-acid battery plates, J. Power Sources 87 (2000) 39.
[8] Z. Tahehara, Dissolution and precipitation reactions of fast charge on the life cycle of positive lead-acid battery plates, J. Power Sources 85 (2000) 29.
[9] D. Pavlov, A theory of the grid/positive active-material(PAM) interface and possible methods to improve PAM utilization and cycle life of lead/acid batteries, J. Power Sources 53 (1995) 9.